Fully Automated Circulating Tumor Cell Isolation Platform with Large-Volume Capacity Based on Lab-on-a-Disc

ARTICLE *in* ANALYTICAL CHEMISTRY · MARCH 2014

Impact Factor: 5.64 · DOI: 10.1021/ac403456t · Source: PubMed

analytical chemistry

Article

pubs.acs.org/ac

Fully Automated Circulating Tumor Cell Isolation Platform with Large-Volume Capacity Based on Lab-on-a-Disc

Jong-Myeon Park,[*,#,†,‡,@] Minseok S. Kim,[*,#,§] Hui-Sung Moon,[†,‡] Chang Eun Yoo,[†,‡] Donghyun Park,[†,‡] Yeon Jeong Kim,[†,‡] Kyung-Yeon Han,[†,‡] June-Young Lee,[∥] Jin Ho Oh,[†] Sun Soo Kim,[⊥] Woong-Yang Park,[‡] Won-Yong Lee,[*,@] and Nam Huh[∥]

[†]Samsung Biomedical Research Institute, Samsung Advanced Institute of Technology, Samsung Electronics Company, Ltd., 81 Irwon-Ro, Gangnam-Gu, Seoul 135-710, Republic of Korea

[‡]Samsung Genome Institute, Samsung Medical Center, Seoul, 135-710, Republic of Korea

[§]Well Aging Research Center, Samsung Advanced Institute of Technology, Samsung Electronics Company, Ltd., San #14-1, Nongseo-dong, Giheung-gu, Yongin-si, Gyeonggi-do, Republic of Korea

[∥]Samsung Advanced Institute of Technology, Samsung Electronics Company, Ltd., San #14-1, Nongseo-dong, Giheung-gu, Yongin-si, Gyeonggi-do, Republic of Korea

[⊥]R&D Solution Lab, Samsung Electronics Company, Ltd, 416, Maetan 3-dong, Yeongtong-gu, Suwon-si, Gyeonggi-do, Republic of Korea

[@]Department of Chemistry and Center for Bioactive Molecular Hybrids, Yonsei University, Seoul 120-749, Republic of Korea

Supporting Information

ABSTRACT: Full automation with high purity for circulating tumor cell (CTC) isolation has been regarded as a key goal to make CTC analysis a "bench-to-bedside" technology. Here, we have developed a novel centrifugal microfluidic platform that can isolate the rare cells from a large volume of whole blood. To isolate CTCs from whole blood, we introduce a disc device having the biggest sample capacity as well as manipulating blood cells for the first time. The fully automated disc platform could handle 5 mL of blood by designing the blood chamber having a triangular obstacle structure (TOS) with lateral direction. To guarantee high purity that enables molecular analysis with the rare cells, CTCs were bound to the microbeads covered with anti-EpCAM to discriminate density between CTCs and blood cells and the CTCs being heavier than blood cells were only settled under a density gradient medium (DGM) layer. To understand the movement of CTCs under centrifugal force, we performed computational fluid dynamics simulation and found that their major trajectories were the boundary walls of the DGM chamber, thereby optimizing the chamber design. After whole blood was inserted into the blood chamber of the disc platform, size- and density-amplified cancer cells were isolated within 78 min, with minimal contamination as much as approximately 12 leukocytes per milliliter. As a model of molecular analysis toward personalized cancer treatment, we performed epidermal growth factor receptor (EGFR) mutation analysis with HCC827 lung cancer cells and the isolated cells were then successfully detected for the mutation by PCR clamping and direct sequencing.

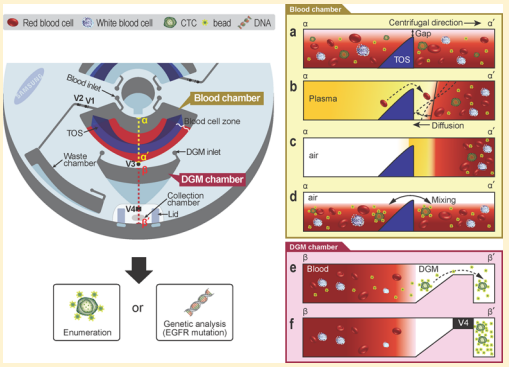

Blood-based cancer diagnostic tools have been spotlighted for their potential in early diagnosis of cancer.[1] Recent findings have reinforced the belief that molecular analysis of circulating tumor cells (CTCs) might play a more crucial role in personalization of cancer treatment than simple enumeration of CTCs.[2] Various methods have been introduced for isolating CTCs, including density gradient separation, nucleic acid-based detection, size filtration, immunomagnetic separation, and separation using multiphysical properties.[3−7] Although each technique may have its own unique advantages, most isolation methods suffer from severe leukocyte contamination (i.e., low purity of isolated CTCs), which is problematic, especially for purposes of genome and transcriptome analyses. Although rigorous washing steps may reduce leukocyte contamination, it can also lead to the loss of isolated CTCs.[8] Therefore, a novel CTC isolation system satisfying high purity without CTC loss is necessary for accurate and reliable molecular analysis.

In addition, although unique CTC isolation techniques are variously presented, as mentioned above, many approaches include sample preprocessing steps to pursue high purity as well as a high recovery rate. The preprocessing helps to reduce isolation time and to improve performance of a CTC capture system because it can significantly reduce final volume from

Received: June 24, 2013
Accepted: March 18, 2014
Published: March 18, 2014

   dx.doi.org/10.1021/ac403456t | *Anal. Chem.* 2014, 86, 3735−3742

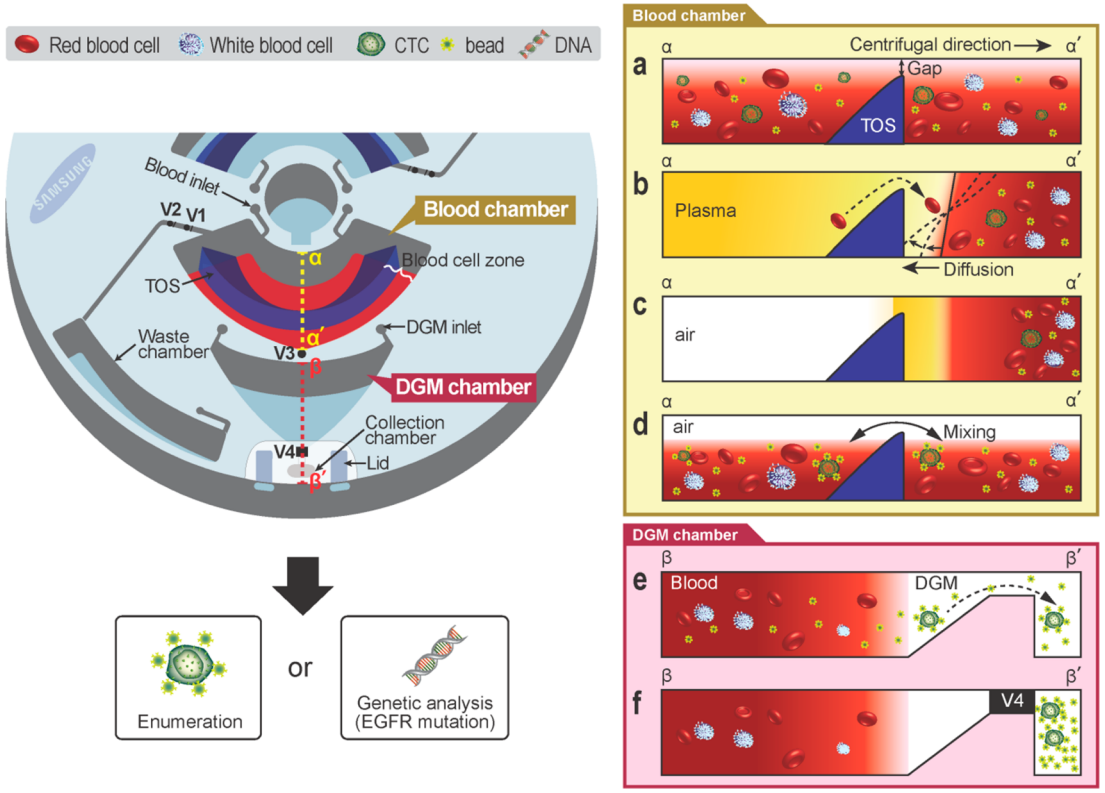

Figure 1. Schematic diagram of the triangular obstacle structure (TOS) disc for CTC isolation. (a) Cross-sectional view of a blood chamber when blood and microbeads are injected via the blood inlet. (b) During centrifugation, blood cells, CTCs, and microbeads are moved to the blood cell zone. (c) To remove plasma, V1 valve is opened and the disc is centrifuged. Then, the area occupying with plasma is changed to air. (d) Mixing process to bind CTCs with microbeads after plasma removal in the blood chamber. (e) Cross-sectional view of a density gradient medium (DGM) chamber after blood transfer. Only CTC-microbead complexes and remnant microbeads larger than the DGM density are moved to the collection chamber. (f) After complete centrifugation, the V4 valve is closed to prevent contamination of blood cells during sample collection. After collecting the sample, CTC enumeration or molecular analysis can be performed.

initial large blood amount and remove blood cells, which play a major role in noise or in blocking particle binding with CTCs. Therefore, density gradient medium (DGM) separation,[9] treatment with blood cell lysis solution,[10] or other biochemical processes[4] are widely utilized before the main isolation process. Since this preprocessing, however, is required for skillful handling and conducted with manual steps, it might make sample-to-sample consistency difficult and reproducibility variable. Thus, full automation in sample preparation is critical in developing a system for rare cell isolation.

As a simple approach that directly utilizes whole blood, microfluidics-based surface capture methods have been vigorously proposed.[11−13] Because they do not require preprocessing to remove erythrocytes and leukocytes, it is relatively straightforward and easy to automate. One of the representative surface capture methods, micropost technique,[12] showed distinguished high purity (over 50%) but a relatively low recovery rate because it depends on the probability of interaction between CTCs and microposts and many erythrocytes interfere with the interaction. To overcome this issue, innovative systems introduced 3D nanostructured substrate[13] and chaotic mixing channels[14] to increase the interaction efficiency of CTCs with antibody anchored on surfaces. Although significantly improving recovery rates by optimizing flow rate, they require relatively large imaging area owing to very long channels and increase processing time according to increased sample volume because of relatively low flow rate and no sample preprocessing steps.

In this paper, we introduce a novel disc-based CTC isolation platform to achieve not only high purity but also realize full automation. To demonstrate the efficacy of this platform, MCF-7 breast cancer cells and HCC827 lung cancer cells were used to model CTCs. We have previously developed several bead-based CTC isolation methods.[4−6] In particular, one approach altering the physical properties (size and density) of CTCs and taking advantage of those altered properties to discriminate them from blood cells demonstrated remarkable performance; however, several manual steps, including plasma removal and DGM separation process, required extensive manual handling and severely limited the robustness of the assay.[5] Therefore, we aimed to fully automate this assay and improve it further to achieve even higher purity toward molecular analysis using isolated CTCs. The process basically requires reagent transfer, removing a portion of the fluids, reagent mixing, and centrifugal force, so that centrifugal microfluidics is eligible to full automation.

Disc-based platforms have widely been studied in various applications,[15] and most of these studies, including our previous works,[16,17] were focused on pathogen detection,[16] immunoassays,[5,17−19] and clinical chemistry.[20] Given that these applications utilize the plasma portion of whole blood, a disc-based platform with limited volume capacity was suitable, since the required volume of blood samples is less than hundreds of microliters. Thus, chambers retaining samples and other reagents do not have to be large. Moreover, since plasma is located on top of the blood cell layer after centrifugation, it is

dx.doi.org/10.1021/ac403456t | Anal. Chem. 2014, 86, 3735−3742

easier to secure enough physical space on a single disc for further processing. On the other hand, when applying centrifugal microfluidics to isolation of CTCs, several technical challenges were encountered, including handling of large fluid volume (5 mL) and manipulation of blood-borne cells, including CTCs.

Given that centrifugal or compact disc (CD)-based microfluidics is inherently limited in physical space that can be used to construct the necessary chambers and channels, large volume handling capability has been considered important in employing this technology to further clinical applications.[15] To the best of our knowledge, only one study demonstrated blood plasma separation with milliliter-scale volume (~ 2 mL) by using multilayer fabrication and siphon valves, but the device may have difficulty securing physical space because the sedimentation chamber itself occupied most of the disc space in the radial direction.[21] As the purpose of our research is to isolate CTCs from whole blood, CD design should consider particle movement (cell transfer) from one chamber to another rather than liquid plasma transfer, as well as manipulation for the higher density of blood cells, which can create spatial limitations for subsequent processes. Toward this end, we have designed a novel disc, composed of a blood chamber with a unique triangular obstacle structure (TOS) that is capable of handling large volumes (~5 mL) and a DGM chamber (Figure 1). The unique TOS in the blood chamber greatly improved retention of all blood cells during the CTC isolation process. The DGM chamber was designed according to computational fluid dynamics (CFD) simulation of cell movement to maximize CTC isolation. The newly developed platform allows "one-click" automation, incorporating all steps of our CTC isolation assay, including plasma separation, plasma removal, microbead binding with CTCs, selective sedimentation of CTCs by passage through the DGM layer, and CTC collection, realizing full automation of CTC isolation from whole blood for the first time. With the final product retrieved from this platform, we can analyze mutation of the EGFR gene by direct sequencing to emphasize the high purity of this platform.

EXPERIMENTAL SECTION

Ethics Statement. Human blood samples were obtained from Yonsei University (Seoul, Korea). Informed written consent was obtained from all participants in all cases, and this study was approved by the Institutional Review Board (IRB) at the Yonsei University, Seoul, Korea.

Materials. Dulbecco's Modified Eagle Medium (DMEM), 4.5 μm diameter superparamagnetic microbeads (Dynamicrobeads Epithelial Enrich), PBS buffer (pH 7.4), fetal bovine serum (FBS), and penicillin−streptomycin were purchased from Invitrogen (Carlsbad, CA). Percoll [pH 8.5−9.5 (25 °C), cell culture tested], paraformaldehyde, Triton X-100, and L-glutamine were obtained from Sigma-Aldrich (St. Louis, MO). 4′,6′-Diamidino-2-phenylindole (DAPI), anticytokeratin fluorescein isothiocyanate (FITC), and anti-CD45 phycoerythrin (PE) were acquired from BD Biosciences (San Jose, CA).

Fabrication of a TOS Disc. The plastic disposable disc is composed of a top and a bottom plate. The top plate has holes for sample injection and air vent, and the bottom plate contains the blood chamber for plasma removal and bead binding (5 mL), the DGM chamber for CTC transport to the collection chamber (5.5 mL), the collection chamber (0.2 mL), and the waste chamber for plasma transfer. The top and bottom plates are made of polycarbonates, and the microfluidic channels and chambers were fabricated using a computer-numerical-controlled process (3D modeling machine; Ideatech corporation, Korea). The detailed procedure of the fabrication and the protocols are described elsewhere.[20,22,23] Briefly, ultriviolet (UV) curable adhesive was applied by silk screen printing on the top plate and followed by dispensing of ferrowax into ferrowax chambers (Figure S1, panels a and b, of the Supporting Information). To assemble the two plates, UV curing was done by applying UV irradiation after the two plates are aligned to face each other (Figure S1c of the Supporting Information). To fabricate normally closed valves, the top plate containing ferrowax was heated by a custom-designed heating system or a laser irradiation system (wavelength: 808 nm, 3 W; Figure S1d of the Supporting Information). When the melted ferrowax flowed into the valve area by capillary phenomenon and changed to solid material (Figure S1e of the Supporting Information), the TOS disc was completely fabricated and ready for use. The principle of the valve operation was described in Figure S2 of the Supporting Information.

Cell Culture and Identification of CTCs. MCF-7 breast cancer and HCC827 lung cancer cell lines were obtained from the American Type Culture Collection (Manassas, VA). Cells were maintained in DMEM supplemented with 10% heat-inactivated FBS, 1% nonessential amino acids, 1% sodium pyruvate, and 1% penicillin/streptomycin solution. Cells were cultured at 37 °C in a humidified atmosphere of 5% CO_2. After the cells reached 80−90% confluence, the medium was removed and replaced with fresh medium. Prior to each experiment, cells grown to confluence were trypsinized and resuspended in their respective growth medium.

For CTC recovery assessments, the sample in the collection chamber was injected into a microfluidic filter utilized in the previous study[5] and the captured CTCs were counted by considering fluorescence staining and morphology. Bright-field, blue, green, and red fluoresencent images were acquired. For MCF-7 cells, the cells that stained positive for cytokeratin (CK, green) and 4′,6-diamidino-2-phenylindole (DAPI, blue) and negative for CD45 (red) were counted as CTCs. For HCC827 cells, on the other hand, they were prestained with CellTracker Green (Molecular Probes, OR), in which labeling was achieved by incubating the cells with the tracking dye (5 μM) for 10 min at room temperature. After washing twice with PBS to remove any excess dye, they were spiked into the whole blood where the actual number of cells in the suspension was determined using the cell counting method, as described previously.[24] In our preliminary study, HCC827 cells showed significant heterogeneity of cytokeratin expression and some part of the cells rarely exhibited the CK fluoresencne signal (see Figure S-3 of the Supporting Information), so that we measured recovery rate of HCC827 cells by the prestaining method instead of anti-CK.[25,26] For HCC827 cells, therefore, green fluorescent, DAPI positive, and CD45 negative cells were counted as CTCs.

To measure the purity of CTCs, the sample in the collection chamber was transferred into an Eppendorf tube followed by removing the supernatant while holding the cell-bead complex with a permanent magnet. The magnetic pellet including CTC-microbead complexes, unbound microbeads, and WBCs were then resuspended in 1 mL of PBS. The solution containing WBCs were inserted into the reservoirs of a 96 well plate, centrifuging the plate with 1000 rpm for 3 min. Then, WBCs that positively stained for DAPI and CD45 were counted by imaging the whole area of reservoirs.

dx.doi.org/10.1021/ac403456t | Anal. Chem. 2014, 86, 3735−3742

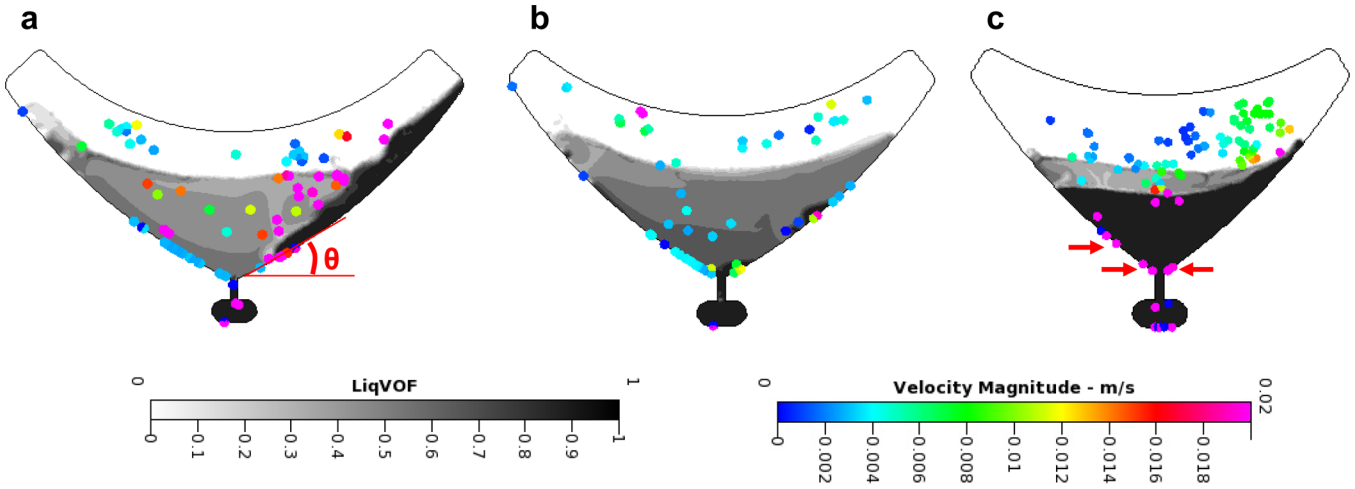

Figure 2. CFD simulation for the movement of particles (CTCs conjugated with microbeads) as the angle of the DGM chamber. Circles in the DGM chamber indicate the CTC particles, including velocity information. In gray scale, black and white colors exhibit DGM and blood, respectively. (a) Angle 30°, 10 s after centrifugation. (b) Angle 40°, 10 s after centrifugation. (c) Angle 50°, 4.7 s after centrifugation. Compared to the lower angles, CTCs showed faster movement at boundary walls toward the collection chamber in this condition (see the arrows), so that they reached to the collection chamber before sufficiently mixing DGM and blood.

Simulation for Cell Movement under Centrifugal Force. CFD simulation was conducted by 2D analysis because the result was not significantly different from that of 3D analysis, which requires much computing power and time. In the CFD-GEOM, grid was created by triangle type meshing, forming 22932 meshes. In the CFD-ACE, three modules (Flow, VOF, and Spray) were simultaneously used with applying rotation effect and transient (auto time step) solving. In addition, we adopted fluid drag force effects to particle movement only, which means that particle movement does not affect fluid flow.

The DGM chamber was modeled with two phases, the blood and DGM layers, to make equal with the experimental condition (DGM: black color; blood: white color in Figure 2). Same with the experiment, blood layer was located on the DGM layer and the area of blood was 1.67 times larger than that of DGM. On the basis of our previous study,[4] the average size of CTCs conjugated with microbeads were set with 22 μm and their average density was assumed with 1130 kg m^{-3}. One hundred particles, representing CTCs with microbeads, were randomly positioned in the blood layer. Since using DGM with 86% Percoll, we measured the viscosity of the DGM by Advanced Rheometer AR 2000 (TA Instruments, DE), and the values for density and viscosity were 1117.6 kg m^{-3} and 6.2 mPa s, respectively. In addition, because the blood transferred to the DGM chamber is removed and as much as about 80% plasma, we measured the viscosity of the blood via the rheometer and the density and viscosity of the blood were decided with 1065 kg m^{-3} and 90 mPa s, respectively. The simulation was calculated by the auto time step method for transient calculation and by using the flow, VOF, and spray modules.

Molecular Analysis. CTCs isolated by the TOS disc were subjected to whole genome amplification (GenomePlex WGA4, Sigma Aldrich), according to the manufacturer's instructions with minor modifications. The modifications were made to minimize the inhibition of the amplification by microbeads. Briefly, cells were separated from microbead before proteinase K treatment. CTC fractions that contained cells and microbeads were suspended in 10 μL of lysis buffer: 50 mM KCl, 1.5 mM $MgCl_2$, 10 mM Tris-HCl (pH 8.3). Cells were detached from microbeads using sonication and the supernatant was transferred to a new tube. Proteinase K in TE buffer was added. After the incubation at 50 °C for 1 h, we followed the manufacturer's instructions. The amplified DNA product was purified with GenElute PCR Cleanup kit (Sigma Aldrich) and quantified by UV absorbance using ND-1000 instrument (NanoDrop Technologies, Rockland, DE). In each sample, EGFR mutation was identified by allele-specific real-time PCR using PNAClamp kit (PNAClamp, Panagene, Korea) and DNA sequencing. For PNAClamp kit, 50 ng of DNA was analyzed with the use of LC480 (LightCycler 480, Roche) real-time PCR system, according to the manufacturer's protocols. Cp (crossing point) value was determined by LightCycler 480 software. For DNA sequencing, EGFR exon 21 region was amplified by a pair of PCR primers: 5′-CAGTGTGATTCGTGGAGCCC-3′ and 5′-CCAGTGCTGTCTCTAAGGGG-3′. The amplified PCR product was purified and analyzed by standard bidirectional DNA sequencing with the use of dye terminator chemistry and a Capillary ABI sequencer (Applied Biosystems).

RESULTS AND DISCUSSION

Design and Operation of the TOS Disc. When patient blood is injected into the blood inlet (Figure 1a), the disc-based CTC isolation process is started with plasma removal. Contrary to that in the conventional centrifugation technique using conical tubes, plasma separation is difficult in the disc approach because centrifugal rotation should be stopped to control the valve on the disc.[23] At this time, the separated blood cells are instantly spread and remixed with the separated plasma because the direction of the blood separation is perpendicular to the gravitational direction. With microliter levels of blood volume, plasma can be separated for a moment by reducing the channel width to delay the diffusion of blood cells.[17] However, when the volume is large (on the order of a few milliliters), separation becomes difficult owing to a limited space. Therefore, we designed a blood chamber with a lateral direction to secure space for the next process. In our observation, separated blood cells moved from the bottom (Figure S-4 of the Supporting Information) owing to gravity; thus, we made a TOS in the

dx.doi.org/10.1021/ac403456t | Anal. Chem. 2014, 86, 3735−3742

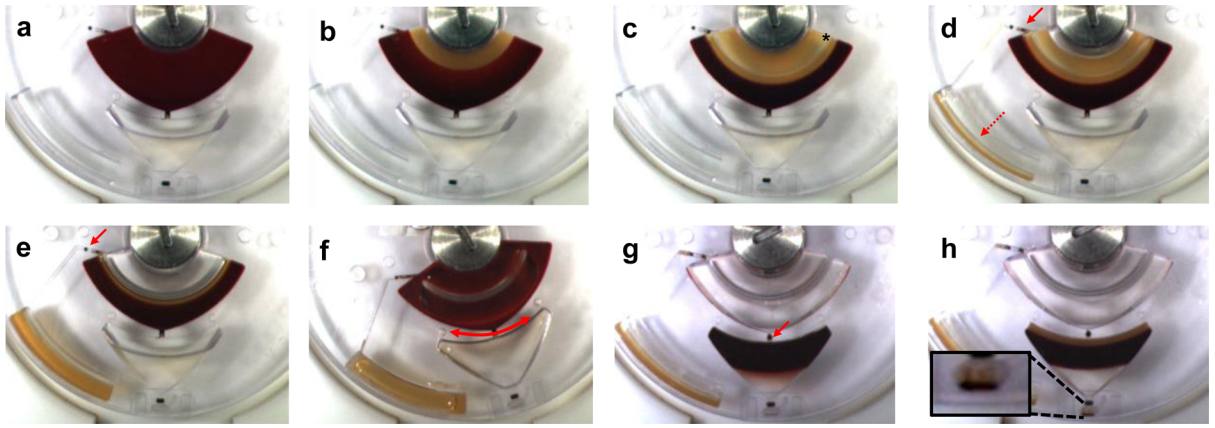

Figure 3. Automated CTC isolation using the TOS disc system. (a) Five milliliters of blood plus microbeads (100 μL) and DGM were injected into the blood and DGM chambers, respectively. (b) During centrifugation, a plasma layer (yellow color) begins to form. (c) After 10 min, the plasma layer now covers the triangular obstacle. Asterisk denotes the position of the triangular obstacle. (d) The plasma is transferred to the waste chamber (dotted arrow) by opening the V1 valve (solid arrow). (e) When the plasma is completely removed, the V2 valve (solid arrow) is closed to prepare for the mixing step. (f) Partial rotation is repeated for the bead binding of the CTCs. (g) A blood layer is formed on the DGM layer by opening the V3 valve (solid arrow), and CTCs and microbeads begin to move down to the collection chamber. (h) After 5 min, the CTCs and microbeads are accumulated in the collection chamber (inset).

blood chamber with a gap not only to move biological particles to the blood cell zone but also to retard the convection of the separated blood cells in the blood cell zone (Figure 1b).

Actually, the height of TOS had trades-off between CTC loss and mixing efficiency. When the height was high, CTC loss was more or less reduced in the plasma removal process. However, it was negatively affected on the bead binding with cancer cells, causing low recovery rate. From the experiment, we determined the height of TOS with 7 mm (2 mm gap) in consideration of low CTC loss and bead coverage of cancer cells. The TOS disc has only 4 valves for a test where V1/V3 and V2/V4 are normally closed and opened valves, respectively (Figure 1). On/off operation of the valves was controlled by laser irradiation where it makes the wax valve melt, thereby changing from solid to the liquid phase.[23] After the plasma is removed (Figure 1c), the mixing process is performed to bind the microbeads with the CTCs (Figure 1d). The mixed blood is transferred to the DGM chamber by opening the V3 valve and CTC-microbead complexes and unbound microbeads only penetrate the DGM layer, arriving at the collection chamber (Figure 1e; sedimentation process). When the disc is stopped, the V4 valve is closed to prevent both contamination of blood cells and CTC loss during removal of the lid and collection of the sample (Figure 1f and Figure S-5 of the Supporting Information). The final product is easily collected by opening the chamber lid (Figure S-6 of the Supporting Information), and we are able to perform CTC enumeration and molecular analysis.

Angle of the DGM Chamber: A Key Parameter for Cell Recovery. It is important to understand the movement of CTCs conjugated with microbeads in the DGM chamber in order to efficiently recover CTCs from the mixture of blood. Therefore, we investigated the particle movement with CFD simulation. Using the fabrication CAD file of the TOS disc, we redraw the parts of the DGM and collection chambers with plane and cross-sectional views. In cross-sectional dimension, particles (CTCs with microbeads) were generally moved along with the bottom planes of the DGM chamber (Figure S-7 of the Supporting Information). From the result, we discovered that the surface roughness of the DGM chamber is important to recover CTCs in the collection chamber, carefully fabricating the bottom plane of the TOS disc to less than 2 μm Ra roughness in the DGM chamber. And also, we simulated particle movement at the plane dimension of the DGM and collection chambers. Interestingly, we found that most of the particles were moved to the collection chamber along the boundary walls of the DGM chamber, meaning that the angle of the DGM chamber is critical for the recovery rate. Therefore, we examined the particle velocity depending on the angle of the DGM chamber (Figure 2). Results revealed that when the angle is higher, not only particles located in the blood cell layer were quickly moved to the bottom of DGM layer but also they showed faster movement at the boundary walls of the DGM chambers (see the arrow of Figure 2c). This simulation result corresponded to the experimental result. Compared to the recovery rate of the DGM chamber having 50° angle, those having 30° and 40° angles were shown to have 25% and 49% recovery rates on average (n = 3), respectively. It is likely that friction force hinders CTC movement toward the collection chamber, thus affecting the recovery rate. As a result, we finally designed the DGM chamber with a 50° angle.

Characterization of Fully Automated TOS Platform. To validate the previously described concept, we tested the isolation process with a homemade disc rotating/laser irradiation system (Movie 1 of the Supporting Information). Figure 3 exhibits the automated CTC isolation process using a TOS disc. Five milliliters of blood and microbeads conjugated with anti-EpCAM were injected into the blood chamber via the blood chamber inlet, and DGM (86% Percoll, 1.8 mL) was inserted to the DGM chamber via the DGM chamber inlet (see Figure 1). The blood and DGM reagent could easily be injected by a 5 mL pipet since the inlet size was tightly fit with the 5 mL pipet tip (Figure 3a). The disc was centrifuged, and a plasma layer began to form (Figure 3b). When the plasma layer was developed over the triangular obstacle (asterisk position of Figure 3c), the blood cell separation process was finished (Figure 3c). At this time, it was important to slowly reduce rotation speed for maintaining the plasma layer, decelerating the disc with about 100 rpm per sec. In our experimental investigation, the separated particles did not go over the

dx.doi.org/10.1021/ac403456t | Anal. Chem. 2014, 86, 3735−3742

triangular obstacle until 30 s after the disc centrifugation was terminated and then the V1 valve for plasma removal was opened within 10 s (see the solid arrow of Figure 3d). The dotted arrow of Figure 3d shows the plasma transferred to the waste chamber. When the plasma was completely removed (Figure 3e), the V2 valve was irradiated with a laser to close the channel between the blood and waste chambers (see the solid arrow of Figure 3e), and the bead-binding process was started by pendular movement where the condition of movement was 150° and 1 Hz for 1 h. After mixing (Figure 3f), the blood was transferred to the DGM chamber by opening the V3 valve (see the solid arrow of Figure 3g). While the centrifugation was maintained for 5 min (450 g), the CTCs conjugated with the microbeads and the remnant microbeads were moved to the collection chamber (see the inset of Figure 3h), and the TOS disc centrifugation was stopped. The detailed spin program was described (Table S-1 of the Supporting Information). When the CTC isolation process was finished, the lid attached on the collection chamber was removed, and the final product was collected with a pipet.

Optimization of the TOS Disc Performance. Beyond CTC enumeration, versatile downstream analysis for extremely low number of CTC such as PCR-based genetic analysis, removal of blood cell contamination is important. To maximize recovery rate and purity, we previously developed a CTC isolation approach that includes 2 sectors: (1) pre-enrichment involving bead binding and selective sedimentation using Ficoll (d = 1.077 g cm^{-3}) and (2) filtration to remove remaining leukocytes and erythrocytes.[5] In our previous study, although good performance in terms of recovery rate was demonstrated and acceptable leukocyte contamination was observed (390 cells mL^{-1}) with selective sedimentation using microbeads, erythrocytes with larger density than leukocytes were severely contaminated with as much as 4.3 × 10^7 cells, which made molecular analysis difficult and caused inaccurate results.[27] As we pursued to directly analyze genetic mutation with the final product of the TOS disc isolation without an additional filtration process, optimization of the DGM and centrifugal condition was necessary for more improved purity. Because the composition of the DGM has a critical impact on blood cell movement to the collection chamber, we examined the blood cell sedimentation as a function of Percoll concentration. On visual examination, red blood cells were found in the collection chamber until 84% (d = 1.115 g cm^{-3}) Percoll, but the collection chamber was clear with 86% (d = 1.118 g cm^{-3}) Percoll. Therefore, we decided to use 86% Percoll as a DGM composition.

Given that one of the most critical processes for high recovery rate is the rotation of the DGM chamber (blood transfer from the blood chamber), we investigated the optimal condition in terms of G-force and time. Figure 4a presents the recovery rate of MCF-7 breast cancer cells (100 spikes) in different centrifugation conditions. It revealed that the two terms, G-force and time, were positively affected on recovery rate as they increased. In addition, we could know that over 90% recovery rate can be achieved when the centrifugal condition was over 300g and 150 s. On the basis of the result, we decided the final centrifugation condition with 450g and 300 s as stable conditions when considering a CTC was bound to only a few microbeads because it requires much centrifugal force and time for sedimentation. We examined the recovery rates of the MCF-7 breast cancer cells and HCC827 lung cancer cells for the condition. Our data indicated that the

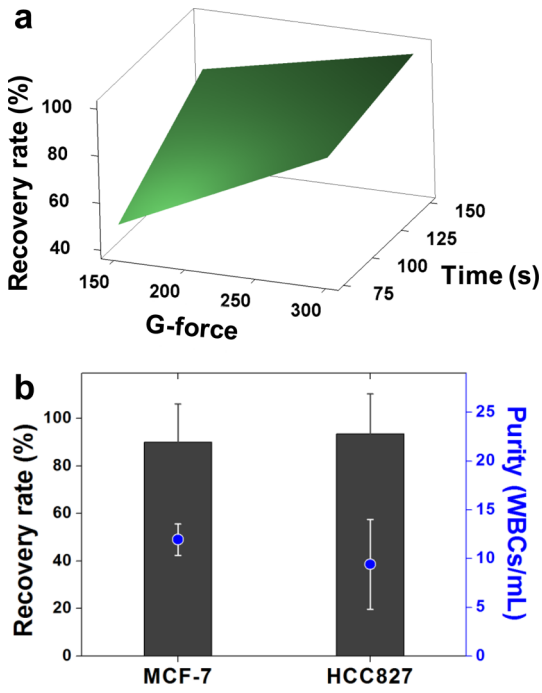

Figure 4. Optimization and performance validation of the TOS disc system. (a) Recovery rate depending on the centrifugation condition (G-force and time) of a DGM chamber. (b) Recovery rates and purities of the MCF-7 and HCC827 cancer cells (n = 3). Experiments were fully automated with the described process, and the centrifugation condition of the DGM chamber was set at 450g and 300 s. All experiments were conducted under 100 spiking cells and 50° angle of the DGM chamber.

recovery rate of MCF-7 cells was similar to that at 300g and 150 s; HCC827 also exhibited a high recovery rate (mean, 95.8%).

Next, we confirmed whether the condition was harmful to cells (Figure S-8 of the Supporting Information). Results revealed that although cell viability decreased depending on spin speed, our working spinning condition was not significantly affected on viability. Control conditions showed around 90% of viability, and the level was maintained until 450g (87% viability in average). However, the cell viability was more or less reduced from 750g (3950 rpm; 77% viability in average). As a result, we counted the leukocytes and erythrocytes in the CTC fraction obtained from the TOS disc without additional washing and found approximately fewer than 12 leukocytes (n = 3, under ± 4.6) and 4.2 × 10^2 erythrocytes (n = 3, ± 41) per milliliters in both cancer cells (Figure 4b).

Analysis of EGFR Mutation for Personalized Medicine. Although genetic mutation has been currently determined by tumor tissues, it is often difficult to obtain tumor tissues through invasive and painful biopsy procedures. Moreover, it sometimes happens that tissue biopsy should be conducted in multiple times since mutation status can change over time and even during the course of therapy. These challenges of tissue biopsy could be potentially overcome by profiling mutation status of CTCs, which is present in the peripheral blood of cancer patients. Detection of genetic mutation in CTCs via minimally invasive biopsies allows monitoring of changes in genetic abnormalities, which could be useful in designing individualized treatment plans for patients. One of the major reasons that molecular characterization of CTCs is technically challenging is that CTCs are extremely rare and difficult to isolate with high purity.

dx.doi.org/10.1021/ac403456t | Anal. Chem. 2014, 86, 3735−3742

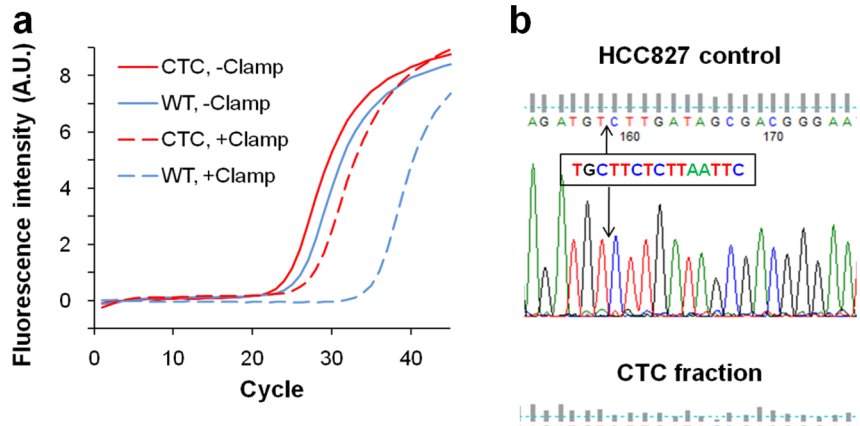

	CTC (*n*=3)	Wildtype (*n*=4)	NTC (*n*=3)
-Clamp Cp	24.7 ± 2.2	24.4 ± 0.8	34.9 ± 1.0
+ Clamp Cp	26.9 ± 0.9	36.4 ± 2.5	36.7 ± 1.9
ΔCp	2.2 ± 2.1	12.0 ± 1.8	1.9 ± 2.5

Figure 5. Detection of the EGFR mutation in the cancer cells isolated by the TOS disc. (a) Genomic DNA from CTC fraction was analyzed by allele-specific real-time PCR analysis using PNA-mediated PCR clamping. Leukocyte genomic DNA was used as a wild-type control. ΔCp represents the Cp difference between with and without PNA clamping. (b) Tracings of the EGFR nucleotide sequencing from the reverse direction. The 15 nucleotides (box) were deleted in the DNAs from the HCC827 cells and CTC fraction. The gray bar indicates the minute wild-type sequence tracing in the chromatogram from the CTC fraction.

To evaluate if the purity and recovery rate of the TOC disc method were sufficient for molecular analysis such as detection of mutations in genomic DNA, we spiked 100 HCC827 lung cancer cells in 5 mL of blood sample, isolated cells using the TOS disc, and detected their deletion mutation in exon 19 of the EGFR gene. To detect the EGFR mutation, the CTC fraction was subjected to cell lysis and whole-genome amplification. Then, the EGFR mutation was analyzed by peptide nucleic acid (PNA)-mediated polymerase chain reaction (PCR) clamping.[28] PNA is a DNA-mimics where the phosphoribose backbone is replaced by a peptide-like repeat of (2-aminoethyl)-glycine units, which offers higher stability to a PNA/DNA hybrid compared with the corresponding DNA/DNA hybrid. Since PNA/DNA hybrid is more destabilized by single base pair mismatches than the corresponding DNA/DNA hybrid, PNA has widely been used to discriminate mutations from wild-type sequences. PNA perfectly matched to wild-type sequences is used to exclude the corresponding wild-type sequences from PCR amplification, whereas it allows PCR amplification of mutant alleles.

As shown in Figure 5a, PNA-mediated EGFR PCR clamping inhibited any detectable amplification from wild-type genomic DNA, based on comparison with no template control (NTC). In contrast, the CTC samples subjected to PNA-mediated PCR clamping were successfully amplified, demonstrating the presence of the mutant sequences in the CTC fractions. The small Cp difference between with and without PNA (ΔCp = 2.2 ± 2.1) indicates that the majority of genomic DNA of the samples are derived from HCC827 cells. Direct sequencing of the amplified PCR products from the CTC fractions (n = 3) clearly displayed the deletion mutation in EGFR exon 19 of HCC827 (Figure 5b),[29] consistently indicating that the HCC827 cells accounted for the majority of the CTC fraction obtained by the TOS disc. Minute leukocyte contamination was indicated by the low amplitude of the wild-type sequence tracing in the chromatogram from the CTC fraction (Figure 5b). We observed little wild-type sequence tracing in the other 2 samples analyzed in this study (data not shown). Overall, our data demonstrated that the CTC fraction obtained by the TOS disc was highly pure and suitable for detection of genetic changes.

CONCLUSIONS

The novel TOS isolation platform satisfies not only full automation but also large-volume capability among centrifugal microfluidics, with high recovery rate and purity. Although many CTC separation studies have been vigorously progressed for a few decades, only the FDA-approved CellSearch system seems to have achieved automation level that can be used in pathology laboratories. However, it also requires an additional manual procedure to separate blood cells from plasma using a centrifuge instrument at the start. On the contrary, it is noted that we could achieve CTC isolation with just one click of a button once a user injects acquired patient blood into a TOS disc with a pipet. Furthermore, we successfully identified EGFR mutation as a model of molecular analyses using CTCs that can potentially be used in clinical practice.

ASSOCIATED CONTENT

Supporting Information

Additional information as noted in text. This material is available free of charge via the Internet at http://pubs.acs.org.

AUTHOR INFORMATION

Corresponding Authors

*E-mail: jong_myeon@samsung.com. Tel: +82-2-3410-2979. Fax: +82-02-3410-7385.

*E-mail: ms0.kim@samsung.com. Tel: +82-31-280-6553. Fax: +82-31-280-9022.
*E-mail: wylee@yonsei.ac.kr. Tel: +82-2-2123-2649. Fax: +82-2-364-7050.

Author Contributions

J.-M.P., M.S.K., W.Y.L., W.P., and N.H. conceived and designed the experiments. J.-M.P., M.S.K., H.S.M., C.E.Y., Y.J.K., and J.Y.L. performed the experiments, and J.-M.P., M.S.K., D.P., J.H.O. analyzed the data. D.P. and K.Y.H. contributed material optimization and supported analysis tools. S.S.K. and M.S.K. performed CFD simulation and analyzed the data. J.-M.P. and M.S.K. wrote the paper, and J.-M.P., M.S.K., and W.Y.L. gave final approval of the manuscript.

Author Contributions

#J.-M.P. and M.S.K. contributed equally to this work.

Notes

The authors declare no competing financial interest.

■ ACKNOWLEDGMENTS

We acknowledge Dr. Seung Il Kim and the contributions of the Yonsei University clinical study participants. This work was supported by the Bio Research Center at the Samsung Advanced Institute of Technology.

■ REFERENCES

(1) Hanash, S. M.; Baik, C. S.; Kallioniemi, O. *Nat. Rev. Clin. Oncol.* **2011**, *8*, 142−150.
(2) Pantel, K.; Alix-Panabieres, C. *Trends Mol. Med.* **2010**, *16*, 398−406.
(3) Paterlini-Brechot, P.; Benali, N. L. *Cancer Lett.* **2007**, *253*, 180−204.
(4) Kim, M. S.; Sim, T. S.; Kim, Y. J.; Kim, S. S.; Jeong, H.; Park, J. M.; Moon, H. S.; Kim, S. I.; Gurel, O.; Lee, S. S.; Lee, J. G.; Park, J. C. *Lab Chip* **2012**, *12*, 2874−2880.
(5) Park, J. M.; Lee, J. Y.; Lee, J. G.; Jeong, H.; Oh, J. M.; Kim, Y. J.; Park, D.; Kim, M. S.; Lee, H. J.; Oh, J. H.; Lee, S. S.; Lee, W. Y.; Huh, N. *Anal. Chem.* **2012**, *84*, 7400−7407.
(6) Kim, M. S.; Kim, J.; Lee, W.; Cho, S. J.; Oh, J. M.; Lee, J. Y.; Baek, S.; Kim, Y. J.; Sim, T. S.; Lee, H. J.; Jung, G. E.; Kim, S. I.; Park, J. M.; Oh, J. H.; Gurel, O.; Lee, S. S.; Lee, J. G. *Small* **2013**, *9*, 3103−3113.
(7) Alix-Panabieres, C.; Schwarzenbach, H.; Pantel, K. *Annu. Rev. Med.* **2012**, *63*, 199−215.
(8) Sieuwerts, A. M.; Kraan, J.; Bolt-de Vries, J.; van der Spoel, P.; Mostert, B.; Martens, J. W.; Gratama, J. W.; Sleijfer, S.; Foekens, J. A. *Breast Cancer Res. Treat.* **2009**, *118*, 455−468.
(9) Dickson, M. N.; Tsinberg, P.; Tang, Z.; Bischoff, F. Z.; Wilson, T.; Leonard, E. F. *Biomicrofluidics* **2011**, *5*, 34119−34134.
(10) Kim, S. J.; Masago, A.; Tamaki, Y.; Akazawa, K.; Tsukamoto, F.; Sato, J.; Ozawa, T.; Tsujino, Y.; Noguchi, S. *Breast Cancer Res. Treat.* **2011**, *128*, 765−773.
(11) Dharmasiri, U.; Njoroge, S. K.; Witek, M. A.; Adebiyi, M. G.; Kamande, J. W.; Hupert, M. L.; Barany, F.; Soper, S. A. *Anal. Chem.* **2011**, *83*, 2301−2309.
(12) Nagrath, S.; Sequist, L. V.; Maheswaran, S.; Bell, D. W.; Irimia, D.; Ulkus, L.; Smith, M. R.; Kwak, E. L.; Digumarthy, S.; Muzikansky, A.; Ryan, P.; Balis, U. J.; Tompkins, R. G.; Haber, D. A.; Toner, M. *Nature* **2007**, *450*, 1235−1239.
(13) Wang, S.; Liu, K.; Liu, J.; Yu, Z. T.; Xu, X.; Zhao, L.; Lee, T.; Lee, E. K.; Reiss, J.; Lee, Y. K.; Chung, L. W.; Huang, J.; Rettig, M.; Seligson, D.; Duraiswamy, K. N.; Shen, C. K.; Tseng, H. R. *Angew. Chem., Int. Ed. Engl.* **2011**, *50*, 3084−3088.
(14) Stott, S. L.; Hsu, C. H.; Tsukrov, D. I.; Yu, M.; Miyamoto, D. T.; Waltman, B. A.; Rothenberg, S. M.; Shah, A. M.; Smas, M. E.; Korir, G. K.; Floyd, F. P., Jr; Gilman, A. J.; Lord, J. B.; Winokur, D.; Springer, S.; Irimia, D.; Nagrath, S.; Sequist, L. V.; Lee, R. J.; Isselbacher, K. J.; Maheswaran, S.; Haber, D. A.; Toner, M. *Proc. Natl. Acad. Sci. U.S.A.* **2010**, *107*, 18392−18397.
(15) Gorkin, R.; Park, J.; Siegrist, J.; Amasia, M.; Lee, B. S.; Park, J. M.; Kim, J.; Kim, H.; Madou, M.; Cho, Y. K. *Lab Chip* **2010**, *10*, 1758−1773.
(16) Cho, Y. K.; Lee, J. G.; Park, J. M.; Lee, B. S.; Lee, Y.; Ko, C. *Lab Chip* **2007**, *7*, 565−573.
(17) Lee, B. S.; Lee, J. N.; Park, J. M.; Lee, J. G.; Kim, S.; Cho, Y. K.; Ko, C. *Lab Chip* **2009**, *9*, 1548−1555.
(18) Park, J.; Sunkara, V.; Kim, T. H.; Hwang, H.; Cho, Y. K. *Anal. Chem.* **2012**, *84*, 2133−2140.
(19) Lai, S.; Wang, S.; Luo, J.; Lee, L. J.; Yang, S. T.; Madou, M. J. *Anal. Chem.* **2004**, *76*, 1832−1837.
(20) Lee, B. S.; Lee, Y. U.; Kim, H. S.; Kim, T. H.; Park, J.; Lee, J. G.; Kim, J.; Kim, H.; Lee, W. G.; Cho, Y. K. *Lab Chip* **2011**, *11*, 70−78.
(21) Amasia, M.; Madou, M. *Bioanalysis* **2010**, *2*, 1701−1710.
(22) Park, J. M.; Lee, J. G. U.S. Patent 8429821 B2, 2013.
(23) Park, J. M.; Cho, Y. K.; Lee, B. S.; Lee, J. G.; Ko, C. *Lab Chip* **2007**, *7*, 557−564.
(24) Hosokawa, M.; Hayata, T.; Fukuda, Y.; Arakaki, A.; Yoshino, T.; Tanaka, T.; Matsunaga, T. *Anal. Chem.* **2010**, *82*, 6629−6635.
(25) Coumans, F. A.; van Dalum, G.; Beck, M.; Terstappen, L. W. *PLoS One* **2013**, *8*, e61774.
(26) Gupta, V.; Jafferji, I.; Garza, M.; Melnikova, V. O.; Hasegawa, D. K.; Pethig, R.; Davis, D. W. *Biomicrofluidics* **2012**, *6*, 24133.
(27) Al-Soud, W. A.; Radstrom, P. *J. Clin. Microbiol.* **2001**, *39*, 485−493.
(28) Orum, H.; Nielsen, P. E.; Egholm, M.; Berg, R. H.; Buchardt, O.; Stanley, C. *Nucleic Acids Res.* **1993**, *21*, 5332−5336.
(29) Helfrich, B. A.; Raben, D.; Varella-Garcia, M.; Gustafson, D.; Chan, D. C.; Bemis, L.; Coldren, C.; Baron, A.; Zeng, C.; Franklin, W. A.; Hirsch, F. R.; Gazdar, A.; Minna, J.; Bunn, P. A., Jr. *Clin. Cancer Res.* **2006**, *12*, 7117−7125.